

Anisotropic magnetization and sign change of dynamic susceptibility in $\text{Na}_{0.85}\text{CoO}_2$ single crystal

Jong-Soo Rhyee^{1,3,*}, J. B. Peng^{1,2}, C. T. Lin^{1,†}, and S. M. Lee³

¹*Max-Planck-Institute for Solid State Research, Heisenbergstrasse 1, Stuttgart, Germany D-70569.*

²*Kunming University of Science and Technology, Yunnan 650093, PR China.*

³*Advanced Materials Lab., Samsung Advanced Institute of Technology, Suwon 440-600, Korea.*

The DC and AC magnetic susceptibilities of $\text{Na}_{0.85}\text{CoO}_2$ single crystals were measured for the different crystal orientations of $H \parallel (\text{ab})$ - and $H \parallel (\text{c})$ -axis. The DC-magnetic susceptibility for $H \parallel (\text{c})$ -direction exhibited the antiferromagnetic transition at $T_N = 22$ K. The thermal hysteresis between the zero-field-cooled (ZFC) and the field-cooled (FC) magnetization below T_N and the large frustration parameter indicated the spin frustration along the c -axis. For an applied magnetic field in $H \parallel (\text{ab})$ -plane, the DC magnetic susceptibility exhibited the logarithmic divergent behavior at low temperatures ($T \leq 6.8$ K). This could be understood by the impurity spin effect, dressed by the spin fluctuation. From the AC magnetic susceptibility measurements, the real part of the AC-susceptibility for $H \parallel (\text{ab})$ exhibited the spin glass-like behavior at low temperatures ($T \leq 4$ K). Remarkably, for an applied AC magnetic field with $H \parallel (\text{c})$ -axis, the sign of the AC magnetic susceptibility changed from a positive to a negative value with increasing AC magnetic field frequency ($f \geq 3$ kHz) at low temperatures ($T \leq 7$ K). We interpret the sign change of AC magnetic susceptibility along the c -axis in terms of the sudden sign reversal of the phase difference ϕ from in-phase to out-of-phase response with an applied AC magnetic field in the AC-susceptibility phase space.

*Corresponding author: js.rhyee@samsung.com (J.S.R.)

†Request for materials should be addressed to: ct.lin@fkf.mpg.de (C.T.L.)

PACS numbers:

I. INTRODUCTION

Since the discovery of superconductivity ($T_c \approx 4.5$ K) in the hydrated compound of $\text{Na}_x\text{CoO}_2y\text{H}_2\text{O}$ ($x \approx 0.35$, $y \approx 1.3$), much attention has been devoted to the Na cobaltate series compounds of Na_xCoO_2 . [1] Nonhydrated compounds of the Na cobaltate system Na_xCoO_2 ($0.3 \leq x \leq 1.0$) exhibit various physical properties depending upon the Na nonstoichiometry, such as high thermoelectric power, [2, 3] quantum criticality, [4] charge ordering, [5, 6] spin density wave, [7] magnetic polaron, [8] *etc.* The variety of physical properties exhibited by this system may originate from the strong correlation among electron, spin, and orbital degrees of freedom. Since few years, intense investigations have been carried out on the magnetic ground state of γ - $\text{Na}_x\text{Co}_y\text{O}_2$ ($0.75 \leq x/y \leq 0.85$, P2 phase) compounds. In the neutron scattering experiments of Na_xCoO_2 ($x = 0.75$ and 0.85) compounds, ferromagnetic interaction was revealed within the CoO_2 layers while antiferromagnetic (AF) ordering was observed perpendicular to the CoO_2 layers (A-type AF). [9, 10] Bulk antiferromagnetism was observed at the Néel temperature $T_N = 19.8$ K along the c -axis in a $\text{Na}_{0.82}\text{CoO}_2$ crystal with two-dimensional antiferromagnetic fluctuation near 30 K. In addition, from the susceptibility, specific heat, and muon spin rotation measurements, a spin density wave was observed, which is an indication of the two-dimensional spin state. [7, 11]

The two-dimensional characteristics of magnetic interaction and various magnetic and electronic ground states

are mainly due to the layered structure of the CoO_2 layer and the unconventional spin state of the Co ion in Na_xCoO_2 . The crystal structure of the CoO_2 sublattice is a triangular network of edge-sharing oxygen octahedra. [12] The magnetic ground state of Na_xCoO_2 is very sensitive with respect to the Na nonstoichiometry. It may be affected by both the charge or the spin state of the Co ion and the crystal structure of the CoO_2 sublattices. The detailed crystal structure variation of Na_xCoO_2 is very complex with respect to Na concentration x . [13] In particular, the $\text{Na}_{0.85}\text{CoO}_2$ crystal is in the upper bound region of the γ -phase $H2$ -type structure. It had the highest value of the Seebeck coefficient in addition to exhibiting the strong spin frustration behavior expected. [3] Significant dynamical spin behavior is usually observed in a strong spin frustration system. Because the strong spin frustration was expected, the measurement of the dynamical spin property would be helpful in understanding the frustration behavior of the $\text{Na}_{0.85}\text{CoO}_2$ compound.

Therefore, we measured the anisotropic DC and AC magnetic susceptibilities of a $\text{Na}_{0.85}\text{CoO}_2$ single crystal in order to study the anisotropic behaviors of the static and dynamic spin response of the Co ion. From the measurement of the DC magnetic susceptibility, it was found that there existed a thermal hysteresis between the zero-field-cooled (ZFC) and the field-cooled (FC) magnetization at low temperatures ($T \leq 20$ K), which implied an unstable magnetic background. On the other hand, an antiferromagnetic (AF) transition was observed at $T_N \approx 22$ K for $(M/H)_c$ along the $H \parallel (\text{c})$ direction. Exotic be-

haviors of $(M/H)_{ab}$ - logarithmic divergent DC magnetic susceptibility at low temperatures ($T \leq 7$ K) and power law dependence $(M/H)_{ab} \propto T^\alpha$ ($\alpha = -0.078$) at high temperatures ($T \geq 100$ K) - were also observed. In addition, from the measurement of the AC magnetic susceptibility, we observed an unconventional sign change from positive to negative of the dynamic spin susceptibility $\chi_c(f, T) \equiv dM_c/dH$ with respect to frequencies and temperatures. In this paper, we have discussed the unusual anisotropic magnetic state and AC frequency response of the dynamic magnetic susceptibility of the $\text{Na}_{0.85}\text{CoO}_2$ crystal.

II. EXPERIMENTAL DETAILS

The single crystalline compound of $\text{Na}_{0.85}\text{CoO}_2$ was grown by the traveling solvent floating zone method using an optical image furnace.[14] The crystal was cleaved into a lamellar hexagonal shape. The chemical concentration of $\text{Na}_{0.85}\text{CoO}_2$ was carefully analyzed by energy dispersive X-ray spectroscopy (EDX) and inductively coupled plasma-atomic emission spectroscopy (ICP-AES). The chemical distribution images by EDX confirmed that the chemical inhomogeneity of the Na ion was less than 2 at.%. The single crystalline property was determined by using the Laue back-scattering and X-ray diffraction techniques. Figure 1 shows well-aligned peaks on the c -axis, perpendicular to the crystal plane; the major sharp $(00l)$ peaks indicate the γ -phase Na_xCoO_2 ($P63/mmc$). The c -axis lattice parameter was determined to be $c = 10.71$ Å from the powder X-ray diffraction measurements. We found a minor impurity phase of α - NaCoO_2 ($R\bar{3}$) of less than 2 at.%. The double phases of γ - and α - Na_xCoO_2 were not extrinsic impurity but intrinsic property in the Na range of $0.85 \leq x \leq 0.95$. [3] The minor phase (less than 2 at.%) of α - NaCoO_2 might not affect the magnetic property because NaCoO_2 is a nonmagnetic material. The temperature-dependent DC magnetization $M(T, H)$ was measured by the magnetic property measurement system (Quantum Design, U.S.A.) in a temperature range of $2 \text{ K} \leq T \leq 300 \text{ K}$ under fixed magnetic fields of $H = 0.1, 1.0, 3.0,$ and 5.0 T. The frequency- and temperature-dependent AC magnetic susceptibilities $\chi(f, T) \equiv dM/dH$ were measured by the Physical Property Measurement System (Quantum Design, U.S.A.) with the AC magnetic susceptometer (ACMS) probe at low temperatures ($T \leq 20$ K) and various frequencies of $0 \text{ Hz} \leq f \leq 10 \text{ kHz}$ with the excitation magnetic field $H_{ex} = 10$ Oe.

III. RESULT AND DISCUSSION

A. Static magnetic susceptibility

Figure 2 presents the temperature-dependent static magnetic susceptibility $M/H(T)$ of $\text{Na}_{0.85}\text{CoO}_2$ under a

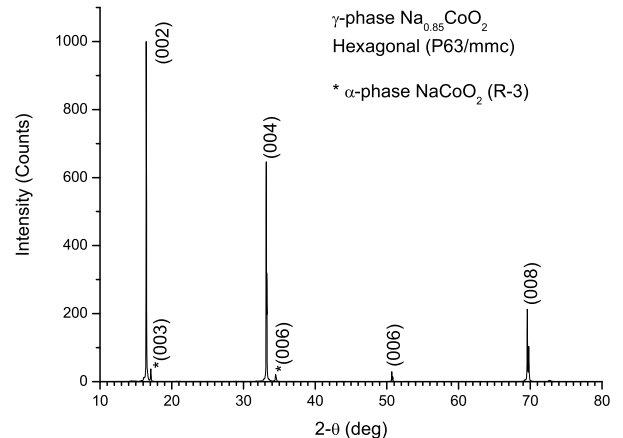


FIG. 1: X-ray diffraction pattern of an $\text{Na}_{0.85}\text{CoO}_2$ single crystal. Major sharp peaks $(00l)$ indicate well-aligned γ -phase Na_xCoO_2 ($P63/mmc$). The minor peaks near 2θ 18° and 34.5° are the (003) and (006) peaks of the α - NaCoO_2 ($R\bar{3}$) impurity phase. The coexistence of the γ and α phases is intrinsic in the Na nonstoichiometry region $0.85 \leq x \leq 0.9$. [3]

magnetic field of $H = 1$ T for different crystal orientations of $H \parallel (ab)$ and $H \parallel (c)$ in the temperature range of $2 \text{ K} \leq T \leq 300 \text{ K}$. The magnetic susceptibility for $H \parallel (c)$ -axis $(M/H)_c(T)$ exhibits an antiferromagnetic (AF) transition at $T_N \simeq 22$ K, which is comparable with that in the case of $\text{Na}_{0.83}\text{CoO}_2$ ($T_N \approx 20$ K). [15] It follows the Curie-Weiss law from 300 K to 150 K as shown in the inset of Fig. 2 (red square, red line). From the Curie-Weiss fitting, the effective magnetic moment and Weiss temperature are estimated to be $\mu_{eff} = 0.91 \mu_B/\text{f.u.}$ and $\Theta_p = -196.8$ K, respectively. Under the assumption of a low spin state (LS), the magnetic moments of Co^{4+} ($3d^5$, $S = 1/2$) and Co^{3+} ($3d^6$, $S = 0$) are $1.732 \mu_B$ and zero, respectively. If we consider only the Co low spin-state, the partial fraction of Co^{4+} is 52 at.%, which is identical to the average valence of Co (3.52). The average Co valence, estimated by the effective magnetic moment, is a little higher than both the $4 - x$ value (3.15) and the value determined by a redox titration. [16] From the wet chemical analysis of the Co valence for $\text{Na}_{0.85}\text{CoO}_2$, the Co valence was estimated to be 3.15. The Co valence higher than our estimation implies that the spin state of Co is not a low-spin state. The spin state transition of the Co ion is widely observed in the cobaltates, for example, perovskite cobaltates $R_{1-x}A_x\text{CoO}_3$ (R : rare earth and A : alkaline earth elements). [17] In this system, the Co^{3+} spin state is changed by the spin state transition from a low-spin (LS, t_{2g}^6 , $S = 0$) to an intermediate-spin (IS, $t_{2g}^5e_g^1$, $S = 1$) or high spin state (HS, $t_{2g}^4e_g^2$, $S = 2$) with respect to temperatures. From the optical conductivity measurement of the $\text{Na}_{0.82}\text{CoO}_2$ single crystal, the charge ordering of Co^{4+} and Co^{3+} was revealed in the CoO_2 layers. [8] The mixed valence of Co^{4+}

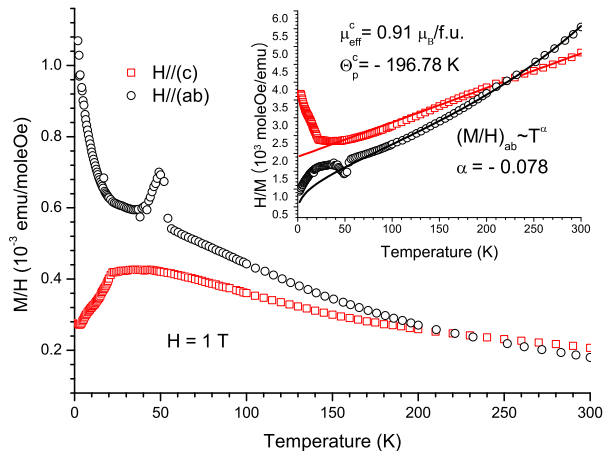


FIG. 2: (Color online) Temperature-dependent DC magnetic susceptibility $(M/H)(T)$ of the $\text{Na}_{0.85}\text{CoO}_2$ single crystal under a static magnetic field $H = 1$ T for different crystal orientations of $H \parallel (ab)$ (black circle) and $H \parallel (c)$ (red rectangle) in the temperature range of $2 \text{ K} \leq T \leq 300 \text{ K}$. Inset shows temperature-dependent inverse DC magnetic susceptibility $(H/M)(T)$. Lines are fitted results of Curie-Weiss law at high temperatures $150 \text{ K} \leq T \leq 300 \text{ K}$ for $H \parallel (c)$ (red line) and power-law behavior with $\chi \sim T^\alpha$ at $T \geq 100 \text{ K}$ for $H \parallel (ab)$ (black line).

and Co^{3+} in cobaltates easily invoke the spin state transition. The Co^{4+} ion lowers the local symmetry of the Co^{3+} ion, which induces the band splitting of the e_g doublet and t_{2g} triplet states. If the energy gap between e_g and t_{2g} orbitals is smaller than the Hund coupling, the intermediate- or high-spin states are favorable because electrons can be transferred from the highest t_{2g} level to the lowest e_g level. The intermediate- or high-spin states of Co^{3+} are not experimentally observed directly. A direct experimental observation of the spin state of Co in $\gamma\text{-Na}_x\text{CoO}_2$ system would be of considerable interest.

The static magnetic susceptibility $(M/H)_{ab}(T)$ under a magnetic field of $H = 1$ T parallel to the (ab)-plane monotonically increases with decreasing temperatures from 300 K to 60 K. With decreasing temperatures, a peak is observed near $T \approx 50 \text{ K}$ with a subsequent increase in susceptibility at low temperatures ($T \leq 10 \text{ K}$). Even though this peak (near 50 K) is sharper than that in the other case,[15] the broad shoulder of $(M/H)_{ab}$ in the intermediate temperature region ($20 \text{ K} \leq T \leq 50 \text{ K}$) is commonly observed for high Na concentration compounds of $\text{Na}_{0.82}\text{CoO}_2$. [11] The authors argue that this may be a signal of a valence fluctuation between Co^{3+} and Co^{4+} . [18] The inverse magnetic susceptibility $(H/M)_{ab}(T)$ (black circle, black line), as shown in the inset of Fig. 2, follows the power-law behavior in the temperature range of $100 \text{ K} \leq T \leq 300 \text{ K}$ according to the following equation: $\chi = \chi_0 + AT^\alpha$, where the zero-temperature susceptibility $\chi_0 = 0.0028$

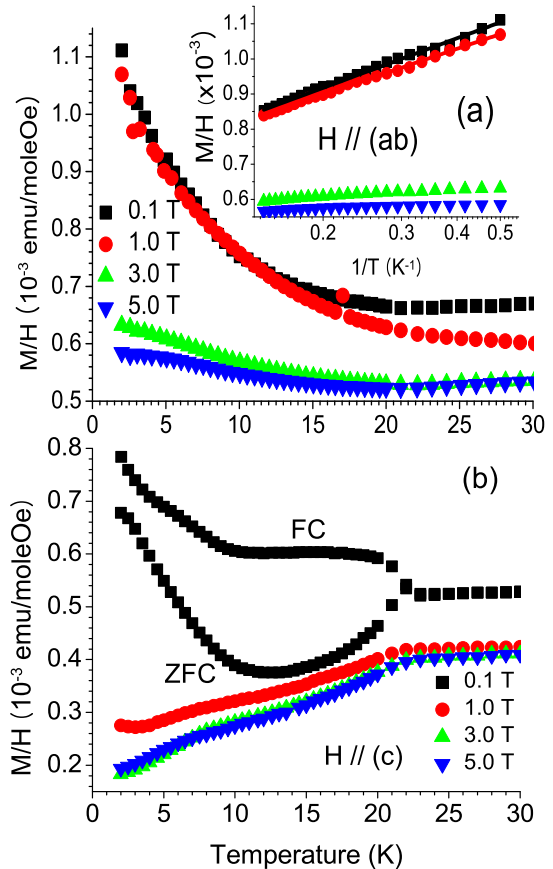


FIG. 3: (Color online) Temperature-dependent DC magnetic susceptibility $(M/H)(T)$ at low temperatures ($2 \text{ K} \leq T \leq 30 \text{ K}$) under static magnetic fields, as indicated, of $H \parallel (ab)$ -axis (a) and of $H \parallel (c)$ -axis (b), respectively. Inset of (a) depicts the logarithmic divergent behavior of the DC magnetic susceptibility $(M/H)_{ab}$ at low temperatures ($2 \text{ K} \leq T \leq 6.8 \text{ K}$) for various magnetic fields, depicted by the semilog plot of M/H vs. $1/T$.

emu/moleOe, pre-factor $A = 0.0046 \text{ emu/moleOeK}$, and power exponent $\alpha = -0.078$. The non-Curie-Weiss behavior of a magnetic ordered system is an indication of the strongly correlated electron behavior. One possible scenario of the power-law behavior in the magnetic susceptibility is the multichannel Kondo effect. [19] The multichannel Kondo model is based on the strong correlation between the local impurity spin and the conduction electron spin. The spins of the conduction electron near the local impurities are paired with a singlet state due to the antiferromagnetic coupling by Pauli matrices. [20] When the total number of electrons overcompensates the local spin $n > 2S$ (where n is the number of degenerate orbital channels and S is the local spin), the power-law or logarithmic divergent behaviors of magnetization, resistivity, or specific heat are observed. The exact solu-

tion of the multichannel Kondo model for dilute impurities show that the magnetic susceptibility should have the power-law dependence with temperatures: $\chi \propto T^\alpha$, where $\alpha = 4/(n+2) - 1$. Under this consideration, the exponent parameter is estimated to be $\alpha = -0.078$ from the magnetic susceptibility $(M/H)_{ab}(T)$ at high temperatures ($T \geq 100$ K). The total number of electron channels n is obtained as $n = 2.34$, which is the case of overcompensation $n > 2S$ (where $S = 1/2$ or 1). The multichannel Kondo effect can be manifested at high temperatures ($T \geq T_K$). [21] In order to clarify the unconventional power-law behavior of $(M/H)_{ab}(T)$ at high temperatures ($T \geq 100$ K), more detailed investigations need to be carried out by using the electrical resistivity, heat capacity, and thermopower measurements.

The logarithmic divergent behavior of $(M/H)_{ab}(T)$ is observed at low temperatures ($T \leq 7$ K), which is different from the Fermi liquid behavior. It may be argued that the impurity spin effect of $(M/H)_{ab}(T)$ is significant due to the symmetrically coupled half-integer spin impurity with the valence fluctuation. Figure 3 (a) shows the temperature-dependent magnetic susceptibility $(M/H)_{ab}(T)$ for different magnetic fields as indicated with $H \parallel$ (ab). The $(M/H)_{ab}(T)$ increases logarithmically at low temperatures ($2 \text{ K} \leq T \leq 7.5 \text{ K}$) as shown in the inset of Fig. 3(a). When an impurity spin S is coupled with an antiferromagnetic background, the sublattice symmetric impurity spin $S = 1/2$ forms a collective spin state of spinon by pulling two spins, resulting in an orthogonal pair of degenerated ground states. If the symmetric impurity spin $1/2$, which is coupled with an antiferromagnetic ground state, is dressed by the valence fluctuation, the impurity spin susceptibility would have a non-Curie divergence given by the following relation: $\chi = \chi_0 + \ln(T^*/T)/T^*$, where T^* ($T \ll T^*$) is the characteristic temperature with the energy scale of $T^* \propto J \exp(-\text{Const}J/g)$ for weak coupling ($g \ll J$) (J is the transfer integral and g is the coupling strength). [22] From the fitting of the above relation, the zero temperature susceptibility χ_0 and characteristic temperature T^* are estimated to be $\chi_0 = 0.0003 \text{ emu/moleOe}$ and $T^* = 10,451.02 \text{ K} = 0.90 \text{ eV}$ for $H = 0.1 \text{ T}$ and $\chi_0 = 0.0004 \text{ emu/moleOe}$ and $T^* = 5,263.16 \text{ K} = 0.45 \text{ eV}$ for $H = 1.0 \text{ T}$. For high magnetic fields ($H = 3 \text{ T}$ and 5 T), the above relation is not fitted. The spin impurity effect is suppressed with increasing magnetic fields as shown in Fig. 3(a). The suppression of the impurity spin effect with increasing magnetic fields might have been caused by the decreasing coupling strength g between the impurity spin and the antiferromagnetic background.

Figure 3(b) depicts the magnetic susceptibility $(M/H)_c$ for $H \parallel$ (c)-axis at low temperatures ($2 \text{ K} \leq T \leq 30 \text{ K}$) for different magnetic fields as indicated. The antiferromagnetic transition $T_N = 22 \text{ K}$ is not changed significantly with increasing magnetic fields. The important feature is the strong thermal hysteresis between the zero-field-cooled (ZFC) and the field-cooled (FC) magnetic susceptibility at $H = 0.1 \text{ T}$ as shown in the Fig.

3(b). While the Néel temperature $T_N = 22 \text{ K}$ is relatively low, the derived value of the Weiss temperature $\Theta_p = -196.78 \text{ K}$ from the Curie-Weiss fitting is very large, which implied a strong antiferromagnetic interaction. The significant discrepancy between the Néel temperature and the Weiss temperature is the evidence of the spin frustration. The frustration parameter, defined by $f = |\Theta_p/T_N|$, is equal to 8.9, which is much larger than that of a conventional antiferromagnet. The antiferromagnetic compounds of Na_xCoO_2 may have the geometrical spin frustration for a wide range of Na concentrations ($x \geq 0.78$) due to the triangular crystal structure of the CoO_2 sublattice. The μSR study of Na_xCoO_2 ($x = 0.78, 0.87, \text{ and } 0.92$) provided the evidence for the strong spin frustration. [23] A small thermal hysteresis between ZFC and FC is also observed for the magnetic susceptibility $(M/H)_{ab}(T)$ with applied magnetic field in the $H \parallel$ (ab)-plane at low temperatures ($T \leq 20 \text{ K}$) under a magnetic field of $H = 0.1 \text{ T}$ (not shown here). The thermal hysteresis between ZFC and FC for different crystal orientations implies the unstable antiferromagnetic background of the $\text{Na}_{0.85}\text{CoO}_2$ compound.

B. Dynamic magnetic susceptibility

In order to study the dynamic spin behavior of this compound, we measured the AC magnetic susceptibility $\chi \equiv dM/dH = \chi' + i\chi''$ for the crystal orientations of both $H \parallel$ (ab)- and $H \parallel$ (c)-axis. Figure 4(a) and (b) represent the temperature-dependent real χ' and imaginary χ'' (insets) parts of the AC magnetic susceptibility for various magnetic field frequencies as indicated with different crystal orientations of $H_{ex} \parallel$ (ab)- and (c)-directions, respectively, where H_{ex} is the excitation AC magnetic field of 10 Oe. Here, the demagnetization factor ($N = 1$) for $H \parallel$ (c) was considered for the following equations because we used the plate-like single crystal.

$$\chi_m = \frac{dM}{dH_a} = \frac{\chi}{1 + N\chi} = \chi'_m + i\chi''_m \quad (1)$$

$$\chi = \frac{dM}{dH} = \frac{\chi_m}{1 - N\chi_m} = \chi' + i\chi'' \quad (2)$$

$$\chi' = \frac{\chi'_m - N(\chi'^2_m + \chi''^2_m)}{N^2(\chi'^2_m + \chi''^2_m) - 2N\chi'_m + 1} \quad (3)$$

$$\chi'' = \frac{\chi''_m}{N^2(\chi'^2_m + \chi''^2_m) - 2N\chi'_m + 1} \quad (4)$$

where χ_m and χ are the measured and intrinsic AC magnetic susceptibilities, respectively.

In the plot of the dynamic magnetic susceptibility χ_{ab} for the $H \parallel$ (ab)-plane, as shown in Fig. 4(a), a broad

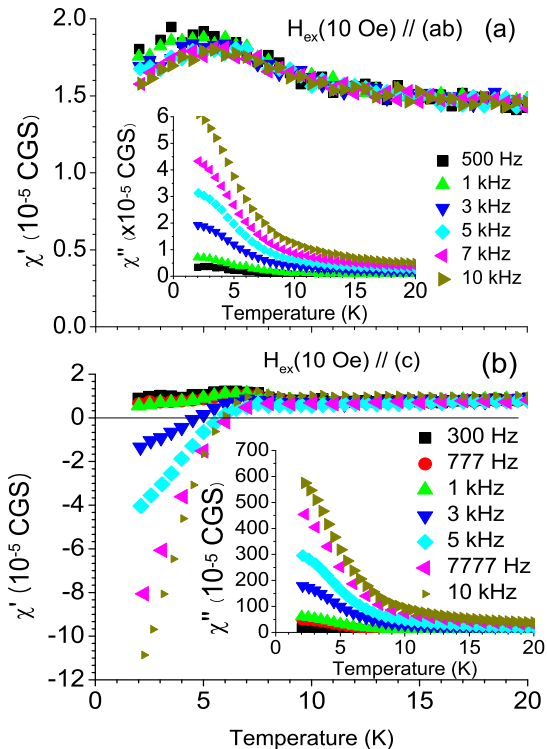


FIG. 4: (Color online) Temperature-dependent real part of the AC magnetic susceptibility $\chi'(T)$ for different excitation field ($H_{ex} = 10$ Oe) frequencies f , as indicated, for $H_{ex} \parallel (ab)$ -axis (a) and $H_{ex} \parallel (c)$ -axis (b), respectively, at low temperatures ($2 \text{ K} \leq T \leq 20 \text{ K}$). Insets of (a) and (b) are the imaginary part of the AC magnetic susceptibility $\chi''(T)$ for the corresponding excitation field frequencies and crystal orientations.

peak is observed near $T_g \approx 4.5$ K for the magnetic field frequency $f = 500$ Hz. With increasing magnetic field frequency, the temperatures at which the broad peak is observed increase slightly from 4.5 K for $f = 500$ Hz to 6.0 K for $f = 10$ kHz. The frequency-dependent antiferromagnetic-like transition of the real part of the AC magnetic susceptibility $\chi'(f, T)$ is not a characteristic of an antiferromagnet but a characteristic of the spin glass-like behavior. The AC magnetic susceptibility behavior χ'_{ab} of the glass-like transition at $T_g \approx 4.5$ K without a phase transition near the antiferromagnetic temperature $T_N = 22$ K is similar to that observed in the case of the $\text{Na}_{0.71}\text{CoO}_2$ compound.[24] The glass freezing temperatures are defined by the cusp points of χ'_{ab} . It is not a conventional spin glass system because of the strong energy dissipation of the AC magnetic susceptibility. The imaginary part of the AC magnetic susceptibility (χ''_{ab}) along the (ab)-plane increases with decreasing temperatures and increasing magnetic field frequencies as shown in the inset of Fig. 4(a). The significant increase in χ''_{ab}

with respect to decreasing temperatures and increasing frequencies is an uncommon behavior of the spin glass system. The out-of-phase part χ'' is much larger than the in-phase part χ' at low temperatures. In a conventional spin glass system, the χ'' has broad peaks near the spin glass transition with a weaker signal than that of χ' . [25, 26] However, in this compound, the energy dissipation part (χ'') of the dynamic spin susceptibility significantly enhanced with decreasing temperatures and increasing frequencies. Therefore, it is concluded that this system is not a simple spin glass system but an exotic system that exhibits strong energy dissipation. Moreover, the real part of the AC magnetic susceptibility χ'_c along the (c)-direction $H \parallel (c)$ exhibits an unconventional sign change from positive to negative with decreasing temperatures ($T \leq 7$ K) and increasing excitation field frequencies ($f \geq 3$ kHz) as shown in Fig. 4(b). This system is quite different from that of the $\text{Na}_{0.71}\text{CoO}_2$ compound as well as the conventional spin glass system.[24] In an usual case, the negative sign of χ' implies a diamagnetic signal. However, this compound is neither a diamagnet nor a superconductor. First, it displays the strong antiferromagnetic transition at $T_N = 22$ K for the $H \parallel (c)$ -axis as shown in Fig. 3(b). Second, like χ'_{ab} , the energy dissipation of magnetic susceptibility χ''_c is very significantly large. Compared to χ''_{ab} (6.0×10^{-5} dimensionless in CGS unit at 2 K and 10 kHz), the value of χ''_c (5.8×10^{-3}) is larger by two orders of magnitude than that of χ''_{ab} . In superconducting materials, the energy dissipation of the dynamic spin susceptibility χ'' diminishes below the transition temperature.

In order to understand the unusual dynamical spin susceptibility behavior of χ_c , we measured the isothermal frequency-dependent AC susceptibility $\chi_c(f)$ at the temperatures of 2 K and 6 K, as shown in Fig. 5(a). With increasing AC field frequency f at $T = 2$ K, $\chi'_c(f)$ decreases and the sign changes at $f \approx 1.8$ kHz. The small peaks at $f = 1.2$ kHz for $T = 2$ K and 6 K have not been understood as yet. The imaginary part of the AC susceptibility $\chi''_c(f)$ increases linearly with increasing AC field frequency, as shown in the inset of Fig. 5(a), which means the linear increase in energy dissipation. The out-of-phase part of the AC susceptibility χ''_c is much more significant than the in-phase part of χ'_c . The sign change of $\chi'_c(f)$ from positive to negative with increasing AC field frequency can be understood by the abrupt sign change of the phase difference ϕ with respect to the AC field frequency. From the definition of AC susceptibility $\chi \equiv \chi' + i\chi'' = \chi_0 \cos \phi + i\chi_0 \sin \phi$, the magnitude of AC susceptibility χ_0 and the phase difference ϕ can be represented by $\chi_0 = \sqrt{\chi'^2 + \chi''^2}$ and $\phi = \arctan(\chi''/\chi')$, respectively. The phase difference ϕ is the relative phase shift between the applied AC magnetic field and the derived magnetic signal. Because the χ'' increases linearly with increasing field frequency f and the orders of magnitude of χ'' is much larger than that of χ' , χ_0 increases linearly with AC field frequencies (not shown). The phase difference ϕ exhibits an abnormal abrupt sign change

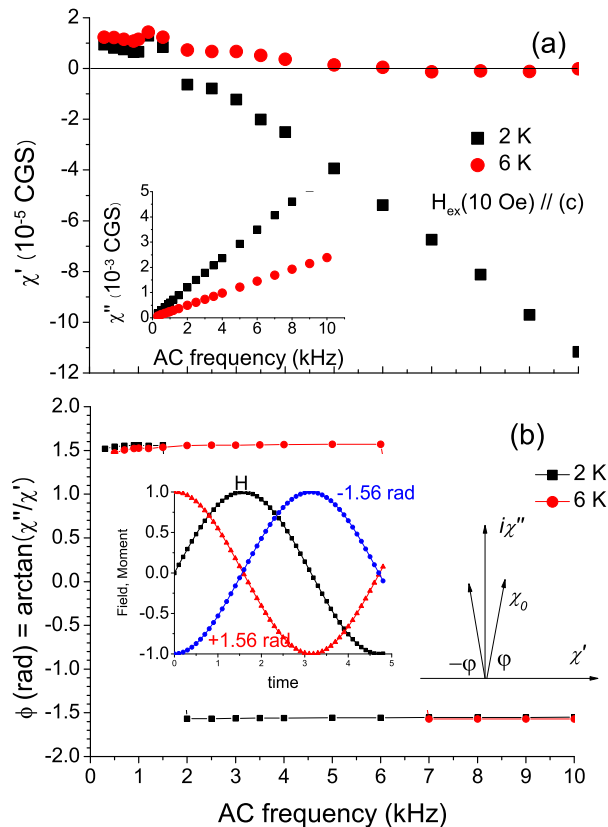


FIG. 5: (Color online) (a): Isothermal frequency-dependent real part $\chi'(f)$ and imaginary part $\chi''(f)$ (inset) AC susceptibilities at constant temperatures $T = 2$ K and 6 K under the excitation field $H_{ex} = 10$ Oe parallel to (c)-direction. (b): Isothermal frequency-dependent phase difference $\phi(f)$, defined by $\arctan(\chi''/\chi')$, at $T = 2$ K and 6 K. Insets of (b) depicts the concept of the sign change of the phase difference ϕ of the dynamic magnetic susceptibility. Right inset of (b) is the magnitude χ_0 and the phase difference ϕ of the dynamic magnetic susceptibility in the complex phase space. Left inset of (b) represents the applied magnetic field (black rectangle) and derived magnetic susceptibility of in-phase (red triangle) and out-of-phase (blue circle) response with time.

from 1.56 rad (89.4°) to -1.56 rad (90.6°) at the frequencies of the χ'_c sign change, as shown in Fig. 5(b). The schematic view of the magnetic susceptibility in the complex phase space is shown in the inset of Fig. 5(b). At low frequencies ($f \leq 1.8$ kHz at $T = 2$ K), these insets exhibit the in-phase response of magnetic susceptibility (red triangle) to the applied AC magnetic field (black rectangle) with $\phi = 1.56$ rad. However, at high frequencies, the phase difference ϕ abruptly changes to -1.56 rad (blue circle) due to a significant increase in the out-of-phase response χ'' . The in-phase to out-of-phase shift of the response of the AC magnetic susceptibility may be a result of the strong energy dissipation χ''_c of this compound. Due to the fact that χ''_c is much larger than χ'_c ,

the phase difference ϕ is on the boundary between the in-phase and the out-of-phase regions in the magnetic susceptibility complex space ($\phi \approx \pi/2$ rad) (right inset of Fig. 5(b)). At present, why the imaginary part of the magnetic susceptibility χ''_c is much stronger than the real part of the susceptibility χ'_c is not clear. The dynamical spin property of this compound may be related to the strong spin frustration in the $H \parallel (c)$ -axis.

IV. CONCLUSION

In summary, we synthesized a high-quality single crystalline compound of $\text{Na}_{0.85}\text{CoO}_2$ by the travelling solvent floating zone method. It was observed from the in-plane and the out-of-plane measurements that the DC magnetic susceptibility showed significant crystal anisotropic properties upon the application of a magnetic field. The DC magnetic susceptibility along the c-axis followed the typical Curie-Weiss behavior with a stable antiferromagnetic transition at $T_N = 22$ K. The strong thermal instability between the zero-field-cooled (ZFC) and the field-cooled (FC) magnetization and the high frustration index indicated a strong spin frustration along the c-axis. The in-plane magnetization exhibited the anomalous power-law behavior at high temperatures ($T \geq 100$ K) and the logarithmic divergent behavior ($\propto \ln(T^*/T)$) at low temperatures ($T \leq 10$ K). The high temperature power-law behavior may be related with the multichannel Kondo effect. The logarithmic divergence can be understood by the impurity spin effect, dressed by the valence fluctuation. Remarkable behavior of the AC magnetic susceptibility was observed at high excitation field frequencies ($f \geq 3$ kHz) along the c-axis. The sign of the real part of the AC magnetic susceptibility along the c-axis changed from positive to negative with decreasing temperatures (near 7 K). We argued that the sign change may due to the abrupt sign change of the phase difference between the applied AC magnetic field and the magnetic susceptibility from 1.56 rad (89.4°) to -1.56 rad (90.6°). Because the imaginary part of the AC magnetic susceptibility was significantly larger than the real part one, the phase difference was on the boundary between the in-phase and the out-of-phase regions. A fundamental question remains as to why the energy dissipation was so significant at high frequencies and low temperatures of this compound. Further investigations would help in clarifying this behavior.

Acknowledgments

We would like to express our sincere gratitude to G. Götz and Christof Busch for their technical assistance.

-
- [1] Kazunori Takada, Hiroya Sakurai, Eiji Takayama-Muromachi, Fujio Izumi, Ruben A. Dilanlan, and Takayoshi Sasaki, *Nature (London)* **422**, 53 (2003).
- [2] Yayu Wang, Nyriisa S. Rogado, R. J. Cava, and N. P. Ong, *Nature (London)* **423**, 425 (2003).
- [3] Minhyea Lee, Liliana Viciu, Lu Li, Yayu Wang, M. L. Foo, S. Watauchi, R. A. Pascal Jr, R. J. Cava, and N. P. Ong, *Nature Materials* **5**, 537 (2006).
- [4] F. Rivadulla, M. Bañobre-López, M. García-Hernández, M. A. López-Quintela, and J. Rivas, *Phys. Rev. B* **73**, 54503 (2006).
- [5] Maw Lin Foo, Yayu Wang, Satoshi Watauchi, H. W. Zandbergen, Tao He, R. J. Cava, and N. P. Ong, *Phys. Rev. Lett.* **92**, 247001 (2004).
- [6] I. R. Mukhamedshin, H. Alloul, G. Collin, and N. Blanchard, *Phys. Rev. Lett.* **93**, 167601 (2004).
- [7] S. P. Bayrakci, I. Mirebeau, P. Bourges, Y. Sidis, M. Enderle, J. Mesot, D. P. Chen, C. T. Lin, and B. Keimer, *Phys. Rev. Lett.* **94**, 157205 (2005).
- [8] C. Bernhard, A. V. Boris, N. N. Kovaleva, G. Khaliullin, A. V. Pimenov, Li Yu, D. P. Chen, C. T. Lin, and B. Keimer, *Phys. Rev. Lett.* **93**, 167003 (2004).
- [9] L. M. Helme, A. T. Boothroyd, R. Coldea, D. Prabhakaran, D. A. Tennant, A. Hiess, and J. Kulda, *Phys. Rev. Lett.* **94**, 157206 (2005).
- [10] L. M. Helme, A. T. Boothroyd, R. Coldea, D. Prabhakaran, A. Stunault, G. J. McIntyre, and N. Kernavainis, *Phys. Rev. B* **73**, 054405 (2006).
- [11] S. P. Bayrakci, C. Bernhard, D. P. Chen, B. Keimer, R. K. Kremer, P. Lemmens, C. T. Lin, C. Niedermayer, and J. Stremper, *Phys. Rev. B* **69**, 100410(R) (2004).
- [12] J. D. Jorgensen, M. Avdeev, D. G. Hinks, J. C. Burley, and S. Short, *Phys. Rev. B* **68**, 214517 (2003).
- [13] L. Viciu, J. W. G. Bos, H. W. Zandbergen, Q. Huang, M. L. Foo, S. Ishiwata, A. P. Ramirez, M. Lee, N. P. Ong, and R. J. Cava, *Phys. Rev. B* **73**, 174104 (2006).
- [14] D. P. Chen, H. C. Chen, A. Maljuk, A. Kulakov, H. Zhang, P. Lemmens, and C. T. Lin, *Phys. Rev. B* **70**, 024506 (2004).
- [15] C. T. Lin, D. P. Chen, J. B. Peng, and P. X. Zhang, *Physica C* **460-462**, 471 (2007).
- [16] Maarit Karppinen, Isao Asako, Teruki Motohashi, and Hisao Yamauchi, *Phys. Rev. B* **71**, 092105 (2005).
- [17] G. Y. Wang, T. Wu, X. G. Luo, W. Wang, and X. H. Chen, *Phys. Rev. B* **73**, 052404 (2006).
- [18] Jong-Soo Rhyee, J. B. Peng, C. T. Lin, and S. M. Lee, *J. Kor. Phys. Soc.* **52**, 391 (2008).
- [19] G. R. Stewart, *Rev. Mod. Phys.* **73**, 797 (2001).
- [20] P. Schlottmann and P. D. Sacramento, *Physica B* **206-207**, 95 (1995).
- [21] S. Pantke and G. R. Stewart, *Solid State Comm.* **108**, 221 (1998).
- [22] David G. Clarke, Thierry Giamarchi, and Boris I. Shraiman, *Phys. Rev. B* **48**, 7070 (1993).
- [23] C. Bernhard, Ch. Niedermayer, A. Drew, G. Khaliullin, S. Bayrakci, J. Stremper, R. K. Kremer, D. P. Chen, C. T. Lin, and B. Keimer, *Euro Phys. Lett.*, **80**, 27005 (2007).
- [24] J. Wooldridge, D. M. K. Paul, G. Balakrishnan, and M. R. Lees, *J. Phys. Condens. Matter* **17**, 707 (2005).
- [25] K. Binder and A. P. Young, *Rev. Mod. Phys.* **58**, 801 (1986).
- [26] N. Hanasaki, K. Watanabe, T. Ohtsuka, I. Kézsmárki, S. Iguchi, S. Miyasaka, and Y. Tokura, *Phys. Rev. Lett.* **99**, 086401 (2007).